

# Powering of cool filaments in cluster cores by buoyant bubbles. I. Qualitative model.

E. Churazov<sup>1,2</sup>, M. Ruszkowski<sup>3,4</sup>, A. Schekochihin<sup>5</sup>

<sup>1</sup> *MPI für Astrophysik, Karl-Schwarzschild str. 1, Garching, D-85741, Germany*

<sup>2</sup> *Space Research Institute, Profsoyuznaya str. 84/32, Moscow, 117997, Russia*

<sup>3</sup> *Department of Astronomy, The University of Michigan, 500 Church Street, Ann Arbor, MI 48109, USA*

<sup>4</sup> *The Michigan Center for Theoretical Physics, 3444 Randall Lab, 450 Church St, Ann Arbor, MI 48109, USA*

<sup>5</sup> *The Rudolf Peierls Centre for Theoretical Physics, University of Oxford, 1 Keble Road, Oxford, OX1 3NP, UK*

Accepted .... Received ...

## ABSTRACT

Cool-core clusters (e.g., Perseus or M87) often possess a network of bright gaseous filaments, observed in radio, infrared, optical and X-ray bands. We propose that these filaments are powered by the reconnection of the magnetic field in the wakes of buoyant bubbles. AGN-inflated bubbles of relativistic plasma rise buoyantly in the cluster atmosphere, stretching and amplifying the field in the wake to values of  $\beta = 8\pi P_{gas}/B^2 \sim 1$ . The field lines in the wake have opposite directions and are forced together as the bubble motion stretches the filament. This setup bears strong similarity to the coronal loops on the Sun or to the Earth’s magneto-tail. The reconnection process naturally explains both the required level of local dissipation rate in filaments and the overall luminosity of filaments. The original source of power for the filaments is the potential energy of buoyant bubbles, inflated by the central AGN.

**Key words:** magnetic reconnection - (galaxies:) quasars: supermassive black holes - galaxies: clusters: intracluster medium - X-rays: galaxies: clusters

## 1 INTRODUCTION

Networks of bright gaseous filaments are ubiquitous in the centres of cool-core clusters (e.g., McDonald et al. 2010).  $H\alpha$  filaments around NGC1275 in the Perseus cluster are perhaps the most famous example (e.g., Minkowski 1957; Lynds 1970). These filaments are observed in many bands/lines, including CO (e.g., Lazareff et al. 1989; Salomé et al. 2006), near-infrared (NIR) lines (Mittal et al. 2012), optical lines (e.g., Conselice, Gallagher, & Wyse 2001) and soft X-rays (Fabian et al. 2003), suggesting a multi-temperature gas sharing approximately the same space within the cluster. For a recent summary of observational results on NGC1275 and M87 filaments, see, e.g., Fabian et al. (2011); Werner et al. (2013) and references therein. Below we discuss NGC1275 and M87 collectively, under the implicit assumption that the same universal mechanism is responsible for the filamentary structures in both objects (and also in other cool-core clusters).

The source of energy powering the filaments is a long-standing problem. The bolometric luminosity of the filaments in the NIR-optical band could be at the level of 10-20% of the total X-ray luminosity of the cluster core.

Various scenarios have been considered, including shocks (David, Bregman, & Seab 1988), photoionization by optical/ultraviolet or X-ray radiation (e.g., Heckman et al. 1989; Voit, Donahue, & Slavin 1994), and thermal conduction (e.g., Boehringer & Fabian 1989). Ferland et al. (2009) argued that the spectra of the outer filaments require the line excitation by energetic particles, although not all line ratios are consistent with this scenario (Mittal et al. 2012). Recently Fabian et al. (2011) and Werner et al. (2013) suggested that the filaments are powered by the hot intracluster medium (ICM), which penetrates into the filaments via turbulent reconnection (see also Soker, Blanton, & Sarazin 2004).

The filaments are long and thin, probably consisting of many threads (Forman et al. 2007; Fabian et al. 2008). This suggests that the magnetic field is playing a role. The role of magnetic fields and in particular magnetic reconnection as a source of energy for filaments has been considered in, e.g., Soker & Sarazin (1990); Jafelice & Friaca (1996); Godon, Soker, & White (1998). It was assumed that an inflow of cooling gas (in the frame of the original cooling flow model, see, e.g. Fabian 1994) increases the magnetic energy density in the core of the cluster. The relative contribution of

the magnetic field to the energy density is further amplified by the radiative cooling losses of the gas thermal energy.

Many models mentioned above appeal to thermal or gravitational energy of the surrounding ICM as the source of energy powering the filaments. Here we consider a different scenario, in which buoyant bubbles of relativistic plasma stretch the magnetic field lines and drive the fields of opposite direction together. In this model the active galactic nucleus (AGN)-inflated bubbles provide the energy that powers the filaments. A schematic picture of this process is shown in Fig. 1.

The structure of this paper is as follows. In §2 we briefly summarize the relevant properties of AGN-inflated bubbles. In §3 we discuss the amplification of the magnetic field by the rising bubbles. In §4 we provide an order-of-magnitude estimate of the rate of energy dissipation by reconnecting magnetic fields in the bubble's tail and the resulting luminosity of the filaments. In §5 we discuss the overall energetics of filaments and other basic properties of our model. Our findings are summarized in §6.

## 2 BUOYANT BUBBLES

Observations suggest that AGN activity regulates the thermal state of the gas by injecting energy into the intra-cluster medium in the cores of relaxed clusters, where radiative cooling time is often as short as few times  $10^8$  yr. AGN jets drive a shock into the ICM and inflate a cocoon of shock-heated material around the nucleus. As the size of the cocoon increases, the expansion velocity becomes subsonic (see, e.g., Heinz, Reynolds, & Begelman 1998). The cocoon transforms into one of several bubbles of relativistic plasma, whose evolution is dominated by the buoyancy force. The cocoon-to-bubble transformation is accompanied by the entrainment of lumps of ambient ICM and subsequent advection of these lumps. The bubbles rise buoyantly through the gaseous atmosphere, leading to a number of spectacular phenomena such as expanding shocks, X-ray-dim and radio-bright cavities, X-ray-dim and radio-dim “ghost” cavities (aged versions of “normal” cavities) and filaments of cool gas in the wakes of the rising bubbles formed by the entrained low-entropy material from the core (Churazov et al. 2000, 2001). With Chandra and XMM-Newton, these features are now studied in great detail in many systems.

Observations further suggest that a large fraction of the energy output of the AGN goes into the enthalpy of the bubbles  $H = \gamma_b P V_b / (\gamma_b - 1)$ , rather than into shocks. Here  $\gamma_b$  is the adiabatic index of the gas inside the bubble ( $\gamma_b = 4/3$  or  $5/3$  depending on whether a relativistic or a non-relativistic gas is considered),  $P$  is the pressure inside the bubble and  $V_b$  is the bubble volume. The partitioning of the AGN energy between shocks and bubble enthalpy depends on the energy injection rate, duration of the AGN outburst and initial conditions (e.g., Forman et al. 2007, , Forman et al. in preparation), but fiducial models predict that about 70% (and certainly more than 50%) goes into the enthalpy of bubbles. Furthermore, the lack of very strong shocks around observed bubbles suggests that the thermal gas pressure of the ICM supporting the bubble can be used in the above

expression for the enthalpy  $H$  (i.e.,  $P \approx P_{gas}$ , the bubble and the ICM are in pressure balance).

The bubbles then serve as a reservoir of potential energy  $\sim H$ , deposited by the AGN. The dynamics of the bubble rise is set by the competition of the buoyancy force and the drag from the ambient gas. Even if we consider only the hydrodynamic drag (i.e., ignoring a possible contribution of magnetic fields) the rise velocity is expected to be subsonic (Churazov et al. 2000). Indeed, the buoyancy force is  $F_b \sim \rho V_b g$ , where  $g$  is the gravitational acceleration, and it is balanced by the ram pressure of the ICM (inertial drag force)  $F_{ram} \sim A \rho v_b^2$ , where  $v_b$  is the bubble's terminal velocity and  $A$  is the cross-section of the bubble. Equating  $F_{ram}$  and  $F_b$  gives  $v_b \sim \sqrt{gR}$ , where  $R$  is the bubble radius. This terminal velocity will be subsonic/transsonic as long as the bubble radius does not exceed the pressure scale height of the atmosphere. Assuming that the bubble is moving subsonically and does not mix with the ambient ICM, the volume of the

bubble expands adiabatically  $V_b = V_{b,0} \left(\frac{P}{P_0}\right)^{-\frac{1}{\gamma_b}}$ , where  $P = P(r)$ ,  $P_0 = P(r_0)$  is the ICM pressure and  $r_0$  and  $r$  are the initial and current distances of the bubble from the cluster centre. For simplicity, we assume below a power-law dependence of the pressure on the radius:  $P = P_0 \left(\frac{r}{r_0}\right)^{-\alpha}$ .

Typically  $\alpha \sim 0.7 - 1$  for the relevant range of radii in cool-core clusters. For example, using radial density and temperature profiles from Churazov et al. (2003) and Forman et al. (2007), we obtained  $\alpha = 0.8$  and  $0.9$  for the Perseus cluster and M87, respectively.

The ambient material and the bubble itself can be threaded by the magnetic fields. As the bubble rises, the magnetic field is amplified, a process discussed in the next section.

## 3 RISE OF THE BUBBLE

The role of magnetic fields in the evolution of buoyant bubbles has been considered in, e.g., Ruszkowski et al. (2007, 2008); O'Neill, De Young, & Jones (2009). Here we concentrate specifically on the threads of the magnetic field in the wake of a rising bubble.

A sketch of the configuration is shown in Fig.1. We assume that the bubble advects a lump of the ICM threaded by magnetic field lines, which are anchored to the gas in the cluster core. We also assume that initially the reconnection of the magnetic field can be neglected (this will be checked in §4). As the bubbles rise, the advected fluid elements and the magnetic field frozen into them are stretched by the bubble motion. We start by considering the evolution of such an advected fluid element occupying a volume  $V \lesssim V_b$ . As the fluid element moves from  $r_0$  to  $r$ , its volume expands adiabatically  $V = V_0 \left(\frac{P}{P_0}\right)^{-\frac{1}{\gamma}}$ , where  $\gamma$  is the adiabatic index of the ICM. The linear size of the stretched fluid element along the direction of motion can be estimated as  $l \approx R_0 + r - r_0$ , where  $R_0$  is the initial size of the fluid element. In the limit  $r \gg r_0$ ,  $l \sim r$ . The cross-section of the fluid element in the

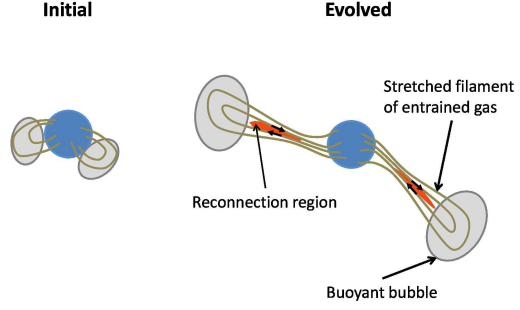
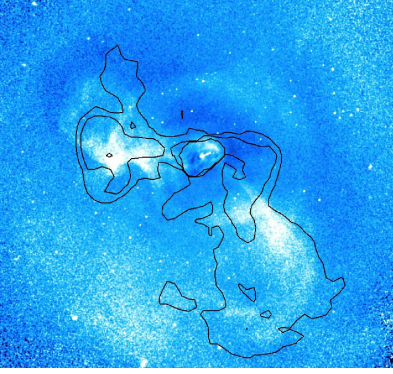


**Figure 1.** Qualitative picture of the current sheets formation by AGN-inflated buoyant bubbles of relativistic plasma, rising in the cluster atmosphere. Nearby elliptical galaxy M87/Virgo is used in this example. **Left:** Morphology of soft X-ray filaments in M87 (Forman et al. 2007) and overall morphology of the radio emitting plasma (Owen, Eilek, & Kassim 2000), superposed as contours. Optical filaments are largely co-spatial with X-ray filaments. Buoyant bubbles rise in the atmosphere, entraining the low-entropy gas from the core (Churazov et al. 2000, 2001) and stretching/squeezing the fluid elements in the wake. Radio emission traces the distribution of the relativistic plasma produced by the AGN. **Right:** Schematic evolution of the magnetic field in the wake. As the bubbles rise, they stretch the magnetic field lines in the entrained fluid elements, thus increasing the strength of the field. The field lines, anchored to the gas in the cluster core, have opposite directions in the wake. They are forced together as the bubble rises. This setup bears strong similarity to the coronal loops on the Sun or to the Earth’s magneto-tail, where reconnection is believed (and, in some cases, observed) to take place.

perpendicular direction is then

$$A \sim \frac{V}{l} \sim \frac{V_0}{l} \left( \frac{P}{P_0} \right)^{-\frac{1}{\gamma}} \sim \frac{V_0}{r} \left( \frac{r}{r_0} \right)^{\frac{\alpha}{\gamma}} \propto r^{\frac{\alpha}{\gamma}-1}. \quad (1)$$

Thus, for  $\alpha < \gamma$ , the cross-section of the fluid element shrinks as the bubble rises.

Here we neglect several effects that might influence the behaviour of rising bubbles. For instance, gas viscosity and/or magnetic fields may affect the development of instabilities at the bubble/ICM interface (e.g., Reynolds et al. 2005; Dong & Stone 2009). We also neglect possible turbulence in the ICM surrounding the entrained fluid elements considered above. Namely, we assume that the stretching velocity of the fluid elements is large enough to dominate over the turbulent ICM motions and/or the overdensity of entrained fluid elements and that their internal magnetic fields help to prevent their disruption. Thus, we assume that entrained fluid elements are evolving solely under the action of stretching due to the bubbles and are approximately adiabatic.

Other potentially important effects are associated with the magnetothermal (MTI; Balbus 2000) and heat-flux-driven buoyancy (HBI; Quataert 2008) instabilities, operating in a stratified weakly magnetized medium. Inside the entrained fluid elements, the magnetic field is mostly radial, while the temperature is decreasing with radius due to adiabatic expansion of the fluid elements. Even if the temperature increases with radius (due to radiative cooling), the stretching velocity is expected to be a large fraction of the sound speed and the velocity of this magnitude is likely to overwhelm the effects of the HBI (Ruszkowski & Oh 2010; Parrish et al. 2010). Therefore, these conditions are not favorable for either MTI or HBI, which can therefore be neglected in this qualitative study.

The stretching of the fluid element will align and amplify the magnetic field  $B$ . From the conservation of the

magnetic flux through the cross-section of the advected fluid element, and using Eq.(1), we find

$$\frac{B}{B_0} \sim \frac{A_0}{A} \sim \frac{l}{R_0} \left( \frac{P}{P_0} \right)^{\frac{1}{\gamma}} \sim \frac{r}{R_0} \left( \frac{r}{r_0} \right)^{-\frac{\alpha}{\gamma}}, \quad (2)$$

where  $B_0$  is the initial magnetic field and  $A_0 \sim V_0/R_0$  the initial cross-section. The corresponding magnetic energy is

$$E_B = \frac{B^2}{8\pi} V \sim \frac{B_0^2}{8\pi} V_0 \frac{l^2}{R_0^2} \left( \frac{P}{P_0} \right)^{\frac{2}{\gamma}} \sim \frac{P_0 V_0}{\beta_0} \frac{r^2}{R_0^2} \left( \frac{r}{r_0} \right)^{-\frac{2\alpha}{\gamma}}, \quad (3)$$

where  $\beta_0 = 8\pi \frac{P_0}{B_0^2} \sim 100$  (e.g., Carilli & Taylor 2002) is the  $\beta$  parameter of the ICM near the initial position of the bubble. Using this expression, we can estimate the maximum distance  $r_{max}$  from the cluster centre that the bubble can reach – this is the radius where the buoyancy force  $F_b \sim \rho V_b g \sim V_b \frac{dP}{dr} \sim V_b \frac{P}{r}$  is equal to  $F_B \sim \frac{dE_B}{dr} \sim \frac{E_B}{r}$ . In the limit of  $r_{max} \gg r_0, R_0$ , the equality  $F_b \sim F_B$  is reached at

$$r_{max} \sim r_0 \left( \beta_0 \frac{V_{b,0}}{V_0} \frac{R_0^2}{r_0^2} \right)^{\frac{1}{2+\alpha-\alpha/\gamma-\alpha/\gamma_b}}. \quad (4)$$

At this radius, the value of  $\beta$  in the stretched fluid element is

$$\beta(r_{max}) \sim \frac{PV}{E_B} \sim \beta_0 \frac{R_0^2}{r_0^2} \left( \beta_0 \frac{V_{b,0}}{V_0} \frac{R_0^2}{r_0^2} \right)^{-\frac{2\gamma+\alpha(\gamma-2)}{2\gamma+\alpha(\gamma-1-\gamma/\gamma_b)}}. \quad (5)$$

Setting  $V_{b,0} \sim r_0^3$  (i.e., initial bubble size is comparable with the initial distance from the cluster centre) and the initial volume of the fluid element  $V_0 \sim R_0^3$ , we get

$$r_{max} \sim r_0 \left( \beta_0 \frac{r_0}{R_0} \right)^{\frac{1}{2+\alpha-\alpha/\gamma-\alpha/\gamma_b}} \sim 10 r_0 \left( \frac{r_0}{R_0} \right)^{0.6} \quad (6)$$

$$\beta(r_{max}) \sim \beta_0 \left( \beta_0 \frac{r_0}{R_0} \right)^{-\frac{2\gamma+\alpha(\gamma-2)}{2\gamma+\alpha(\gamma-1-\gamma/\gamma_b)}} \frac{R_0^2}{r_0^2} \sim \left( \frac{r_0}{R_0} \right)^{-3}, \quad (7)$$

where the last expressions have been obtained for a set of

fiducial values  $\alpha \sim 0.85$ ,  $\gamma = 5/3$ ,  $\gamma_b = 4/3$ ,  $\beta_0 \sim 100$ . Thus, taking  $r_0 \sim R_0$ , it is reasonable to expect the bubble to rise a distance of order  $r \sim 10 r_0$  before the buoyancy and magnetic forces come into balance. At this point, the  $\beta$  parameter in the stretched fluid elements approaches unity. Circumstantial evidence for the magnetic field energy density comparable to the ICM thermal pressure was indeed presented (based on a different argument) in Fabian et al. (2011); Werner et al. (2013).

#### 4 RECONNECTION IN THE FILAMENTS

Once the bubble is at  $r_{max}$ , further stretching of the field lines is not possible. The bubble (or fluid elements attached to it) would “hang” on the magnetic field lines. However, the field lines in the stretched fluid elements will have opposite directions and are forced together by the shrinking cross-section of the filament. The configuration bears strong similarity to the solar coronal loops (e.g., Kopp & Pneuman 1976) or the Earth magneto-tail (e.g., Nishida 2000), making the filament prone to reconnection. As the anti-parallel field lines come together, current sheets are formed, with an inflow of magnetic energy, which is eventually dissipated there. The release of magnetic energy allows the bubble to rise further.

Magnetic reconnection in both collisional (MHD) and collisionless plasmas proceeds at a rate that is independent of Ohmic resistivity (Uzdensky, Loureiro, & Schekochihin 2010) or other aspects of plasma microphysics (Rogers et al. 2001). Namely, one can write a rough estimate of the magnetic energy inflow per unit surface of the reconnecting layer as follows:

$$L_{rec} \approx \epsilon v_A \frac{B^2}{8\pi}, \quad (8)$$

where  $v_A = \sqrt{\frac{B^2}{4\pi n \mu m_p}}$  is the Alfvén speed,  $n$  is the gas particle density,  $\mu$  mean particle atomic weight and  $\epsilon$  is the dimensionless reconnection rate between  $\epsilon \sim 0.01$  for collisional plasmas (Uzdensky, Loureiro, & Schekochihin 2010; Loureiro et al. 2012; Bhattacharjee et al. 2009; Daughton et al. 2009; Loureiro et al. 2009) and  $\epsilon \sim 0.1$  for collisionless ones (Birn et al. 2001).

Using this expression, we can compare the increase of the magnetic energy due to stretching  $\frac{dE_B}{dt} \sim F_B v_b$  and the release of the magnetic energy due to reconnection  $\left(\frac{dE_B}{dt}\right)_{rec} \sim S L_{rec}$ . Here  $F_B \sim E_B/r$ ,  $v_b \sim \sqrt{gR} \sim c_s \sqrt{V_b^{1/3}/r}$  is the velocity of the bubble,  $c_s$  is the speed of sound (note  $v_A \sim c_s/\sqrt{\beta}$ ) and  $S$  is the lateral area of the filament. This area can be estimated as the product of the length of the filament  $\sim r$  and its transverse size  $\sim \sqrt{V}/r$ . Using the results of Sec.3 and our fiducial values of  $\alpha$ ,  $\gamma$ ,  $\gamma_b$ , we can estimate the radius  $r_{eq}$  where the rates of generation and dissipation of magnetic energy are approximately equal:

$$r_{eq} \sim r_0 \left(\frac{\epsilon}{\eta\sqrt{\beta_0}}\right)^{-0.4} \left(\frac{r_0}{R_0}\right)^{-1} \sim (6 - 16)r_0, \quad (9)$$

depending on the reconnection rate  $\epsilon$ . This is close to the radius  $r_{max}$  where  $\beta \sim 1$ . For  $r < r_{eq}$ , reconnection is slow relative to field stretching, so it was reasonable in §3 to ignore the former.

Assuming that  $\beta \sim 1$ , we can replace the magnetic energy density with the thermal energy density  $\frac{B^2}{8\pi} \sim nkT$  and the Alfvén velocity  $v_A$  with the sound speed  $c_s = \sqrt{\gamma \frac{P_{gas}}{\mu m_p}}$ .

This gives an order-of-magnitude estimate of the surface influx of energy<sup>1</sup>:

$$L_{rec} \approx \epsilon c_s nkT. \quad (10)$$

For the NGC1275 and M87 the estimates of the total emitted surface flux by the filaments are available (Fabian et al. 2011; Werner et al. 2013):  $L_{em} \sim 10^{-2}$  ergs s<sup>-1</sup> cm<sup>-2</sup>  $\sim 0.2c_s nkT$  and  $\sim 2.2 \cdot 10^{-3}$  ergs s<sup>-1</sup> cm<sup>-2</sup>  $\sim 0.1c_s nkT$  respectively. Thus there is an interesting order-of-magnitude agreement between the amount of energy that can be produced by fast reconnection and the amount of energy emitted by the filaments, i.e.  $\frac{L_{rec}}{L_{em}} \approx \frac{\epsilon}{0.1}$ . If the reconnection rate is on the stronger side of the possible values, viz.  $\epsilon \sim 0.1$ , the energy release from reconnection is comparable to the cooling losses of the filaments.

The evolution of buoyant bubbles in a magnetized ICM has been considered in several numerical simulations (e.g., Robinson et al. 2004; Ruszkowski et al. 2007, 2008; O’Neill, De Young, & Jones 2009; Dong & Stone 2009). Most of these studies are focused on the overall dynamics of the rising bubbles, rather than on the structure of the magnetic field in the wake and associated reconnection. We will address these issues in subsequent publications. Nevertheless, some of the features relevant for our discussion can be found in existing simulations, especially in configurations where magnetic field lines are threading the bubble and are anchored to the ambient ICM. For example, enhanced fields in the wake are seen in the 2D simulations of Robinson et al. (2004) with an initially horizontal magnetic field. In Ruszkowski et al. (2007), the wake behind the bubble shows a narrow layer of close-to-zero magnetic field which is likely the area of anti-parallel magnetic fields, where reconnection is likely to happen.

#### 5 DISCUSSION

The overall energetics of the cool cores are believed to be determined by the balance of the AGN activity and gas cooling. In other words, one can assume that the cooling losses are approximately matched by the amount of mechanical energy pumped by the AGN into the gas in the form

<sup>1</sup> Note that while the dissipation rate of the magnetic energy in the reconnection process does not have to be the same as the reconnection rate, it is reasonable to expect that they are comparable (there is some numerical evidence in support of this, e.g., Loureiro et al. 2012). In our simple estimates we have absorbed both the reconnection and the dissipation rate into the  $\epsilon$  parameter.



of relativistic bubbles. Observations suggest that a significant (if not dominant) fraction of the AGN energy goes into the enthalpy of the bubbles rather than into shocks (e.g., Churazov et al. 2002). This means that potential energy of underdense bubbles created by the AGN per unit time approximately matches gas cooling losses. The estimates in §3 suggest that by the time  $\beta$  reaches 1, the bubble has moved to  $r_{max} \sim 10r_0$ . Let us estimate the ratio  $f_B$  of the magnetic energy of the stretched fluid element at this moment to the initial enthalpy of the bubble  $H_0 = \frac{\gamma_b}{\gamma_b - 1} P_0 V_{b,0}$ :

$$f_B = \frac{E_B(r_{max})}{H_0} \sim \frac{\gamma_b - 1}{\gamma_b} \frac{1}{\beta(r_{max})} \frac{PV}{P_0 V_{b,0}} \sim \frac{\gamma_b - 1}{\gamma_b} \frac{1}{\beta(r_{max})} \left(\frac{r_{max}}{r_0}\right)^{-\alpha \frac{\gamma_b - 1}{\gamma_b}} \left(\frac{R_0}{r_0}\right)^3 \sim 0.1, \quad (11)$$

using eq.(3,7,6) and neglecting dependence on  $R_0/r_0$ . At the same time, the fraction of enthalpy remaining in the bubble is

$$f_H = \frac{H(r_{max})}{H_0} = \frac{PV_b}{P_0 V_{b,0}} \sim \left(\frac{r_{max}}{r_0}\right)^{-\alpha \frac{\gamma_b - 1}{\gamma_b}} \sim 0.5. \quad (12)$$

The rest of the initial enthalpy has already been transferred to the gas via hydrodynamic drag, potential energy of the uplifted gas, magnetic energy, and excitation of  $g$ -modes, which then dissipate in the ICM (Churazov et al. 2002). Comparison of  $f_H$  and  $f_B$  suggests that by the time the bubble reaches  $r_{max}$ , about 20% of its available energy will have gone into magnetic energy forced into its tail. The luminosity of the filaments from NIR to optical bands amounts to 10-20% of the bolometric luminosity of the cluster cores. This means that 10-20% of the potential energy available conversion into magnetic energy should indeed go into reconnection and the associated heating. When the reconnection releases magnetic energy, the bubble continues to rise beyond  $r_{max}$ .

Note that it is very likely that in real clusters, there is a considerable spread in the values of initial parameters, such as, e.g.,  $\beta_0$ ,  $r_0/R_0$ . This suggests a large variation in the appearance of the filaments in different clusters or even of filaments/bubbles in the same cluster.

In our simple scenario, only the regions where the configuration of magnetic field is favorable to reconnection are observed as filaments. The energy of the magnetic field is the principal source of energy for the outer filaments, rather than ICM thermal energy or photoionization, although both can contribute. The implication is that the filaments need not necessarily grow in mass with time, instead they thermalize and emit the bubble energy mediated by magnetic fields.

The cooling of the gas is not the central element of our model (cf. Soker & Sarazin 1990; Jafelice & Friaca 1996) in the sense that the main driver of the reconnection is the stretching of the field lines by the bubbles rather than the loss of thermal energy by the cooling gas. It is nevertheless clear that a large amount of cool gas is present in these systems. In the simplest scenario, this gas intercepts, thermalizes and re-emits the released energy of the magnetic field. The discussion of how the magnetic energy is split be-

tween the kinetic energy of the gas, its thermal energy and non-thermal particles, or of the actual excitation of the optical lines is beyond the scope of this Letter. We nevertheless note that the presence of non-thermal particles may help explain many properties of the emission spectra (Ferland et al. 2009).

As a speculative extension of our qualitative model, we note that the gas leaving the reconnection region will have velocities of order  $v_A$ , i.e., close to the sound speed (because  $\beta \sim 1$ ). The outflow is typically bi-directional, i.e., along the filaments. Reconnection in extended current sheets is typically accompanied by generation and ejection of copious numbers of plasmoids (Loureiro et al. 2012; Bhattacharjee et al. 2009; Daughton et al. 2009; Samtaney et al. 2009), some of them very large (Loureiro et al. 2012). If the filament is aligned along the line of sight towards an observer, this may lead to the appearance of gas lumps moving towards the core, away from the observer with the speed that can be as large as  $\sim 10^3 \text{ km s}^{-1}$  for the hot gas. There is a so-called High Velocity system (HV) in the core of the Perseus cluster – a line-emitting region in the core of NGC1275, with a recession velocity  $\sim 3000 \text{ km/s}$  larger than the systemic velocity of NGC1275 (e.g., Minkowski 1957), which is nevertheless located in front of NGC1275 (e.g., De Young, Roberts, & Saslaw 1973) and, therefore, is moving towards the nucleus. While the infall velocity of HV seems to be too large for a conceivable plasmoid-ejection mechanism, it is nevertheless interesting to note that in some favorable configurations, high-velocity gas lumps can be observed.

## 6 CONCLUSIONS

We argue that buoyant bubbles in the cores of galaxy clusters stretch the fluid elements advected from the core, forming gaseous filaments and aligning and amplifying the magnetic field in these filaments. The field grows to  $\beta \sim 1$  after the bubbles rise a distance of the order of 10 times their initial size. The field lines in the wake of the bubble are anti-parallel and are forced together. This setup bears strong similarity to the coronal loops on the Sun or to the Earth's magneto-tail. The reconnection process can naturally explain both the required local dissipation rate in filaments and the overall energy balance. In this model, the original source of power for the filaments is the potential energy of buoyant bubbles, inflated by the central AGN. Of the order of 10% of the total mechanical energy deposited by the AGN in the form of such relativistic bubbles can be converted into the emission from the filaments.

## 7 ACKNOWLEDGMENTS

EC acknowledges useful discussions with A.Petrukovich and H.Spruit. This work was supported in part by the Leverhulme Trust Network on Magnetized Plasma Turbulence and the programme OFN-17 of the Division of Physical Sciences of the Russian Academy of Science. MR acknowledges

NSF grant AST 1008454 and NASA ATP grant 12-ATP12-0017.

## REFERENCES

- Balbus S. A., 2000, *ApJ*, 534, 420
- Bhattacharjee A., Huang Y.-M., Yang H., Rogers B., 2009, *PhPl*, 16, 112102
- Birn J., et al., 2001, *JGR*, 106, 3715
- Boehringer H., Fabian A. C., 1989, *MNRAS*, 237, 1147
- Carilli C. L., Taylor G. B., 2002, *ARA&A*, 40, 319
- Churazov E., Forman W., Jones C., Böhringer H., 2000, *A&A*, 356, 788
- Churazov E., Brüggén M., Kaiser C. R., Böhringer H., Forman W., 2001, *ApJ*, 554, 261
- Churazov E., Sunyaev R., Forman W., Böhringer H., 2002, *MNRAS*, 332, 729
- Churazov E., Forman W., Jones C., Böhringer H., 2003, *ApJ*, 590, 225
- Conselice C. J., Gallagher J. S., III, Wyse R. F. G., 2001, *AJ*, 122, 2281
- Daughton W., Roytershteyn V., Albright B. J., Karimabadi H., Yin L., Bowers K. J., 2009, *PhRvL*, 103, 065004
- David L. P., Bregman J. N., Seab C. G., 1988, *ApJ*, 329, 66
- De Young D. S., Roberts M. S., Saslaw W. C., 1973, *ApJ*, 185, 809
- Dong R., Stone J. M., 2009, *ApJ*, 704, 1309
- Fabian A. C., 1994, *ARA&A*, 32, 277
- Fabian A. C., Sanders J. S., Crawford C. S., Conselice C. J., Gallagher J. S., Wyse R. F. G., 2003, *MNRAS*, 344, L48
- Fabian A. C., Johnstone R. M., Sanders J. S., Conselice C. J., Crawford C. S., Gallagher J. S., III, Zweibel E., 2008, *Nature*, 454, 968
- Fabian A. C., Sanders J. S., Williams R. J. R., Lazarian A., Ferland G. J., Johnstone R. M., 2011, *MNRAS*, 417, 172
- Ferland G. J., Fabian A. C., Hatch N. A., Johnstone R. M., Porter R. L., van Hoof P. A. M., Williams R. J. R., 2009, *MNRAS*, 392, 1475
- Forman W., et al., 2007, *ApJ*, 665, 1057
- Godon P., Soker N., White R. E., III, 1998, *AJ*, 116, 37
- Heckman T. M., Baum S. A., van Breugel W. J. M., McCarthy P., 1989, *ApJ*, 338, 48
- Heinz S., Reynolds C. S., Begelman M. C., 1998, *ApJ*, 501, 126
- Jafelice L. C., Friaca A. C. S., 1996, *MNRAS*, 280, 438
- Kopp R. A., Pneuman G. W., 1976, *SoPh*, 50, 85
- Lazareff B., Castets A., Kim D.-W., Jura M., 1989, *ApJ*, 336, L13
- Loureiro N. F., Samtaney R., Schekochihin A. A., Uzdensky D. A., 2012, *PhPl*, 19, 042303
- Loureiro N. F., Uzdensky D. A., Schekochihin A. A., Cowley S. C., Yousef T. A., 2009, *MNRAS*, 399, L146
- Lynds R., 1970, *ApJ*, 159, L151
- McDonald M., Veilleux S., Rupke D. S. N., Mushotzky R., 2010, *ApJ*, 721, 1262
- Minkowski R., 1957, *IAUS*, 4, 107
- Mittal R., et al., 2012, *MNRAS*, 426, 2957
- Nishida A., 2000, *SSRv*, 91, 507
- O’Neill S. M., De Young D. S., Jones T. W., 2009, *ApJ*, 694, 1317
- Owen F. N., Eilek J. A., Kassim N. E., 2000, *ApJ*, 543, 611
- Parrish, I. J., Quataert, E., & Sharma, P. 2010, *ApJL*, 712, L194
- Quataert E., 2008, *ApJ*, 673, 758
- Reynolds C. S., McKernan B., Fabian A. C., Stone J. M., Vernaleo J. C., 2005, *MNRAS*, 357, 242
- Robinson K., et al., 2004, *ApJ*, 601, 621
- Rogers B. N., Denton R. E., Drake J. F., Shay M. A., 2001, *PhRvL*, 87, 195004
- Ruszkowski M., Enßlin T. A., Brüggén M., Heinz S., Pfrommer C., 2007, *MNRAS*, 378, 662
- Ruszkowski M., Enßlin T. A., Brüggén M., Begelman M. C., Churazov E., 2008, *MNRAS*, 383, 1359
- Ruszkowski, M., & Oh, S. P. 2010, *ApJ*, 713, 1332
- Salomé P., et al., 2006, *A&A*, 454, 437
- Samtaney R., Loureiro N. F., Uzdensky D. A., Schekochihin A. A., Cowley S. C., 2009, *PhRvL*, 103, 105004
- Soker N., Sarazin C. L., 1990, *ApJ*, 348, 73
- Soker N., Blanton E. L., Sarazin C. L., 2004, *A&A*, 422, 445
- Spruit H. C., 2013, preprint(arXiv:1301.5572)
- Uzdensky D. A., Loureiro N. F., Schekochihin A. A., 2010, *PhRvL*, 105, 235002
- Voit G. M., Donahue M., Slavin J. D., 1994, *ApJS*, 95, 87
- Werner N., et al., 2013, *ApJ*, 767, 153